Power hardware in-the-loop laboratory test environment for small scale wind turbine prototype

A.S. Mäkinen, T. Messo, H.Tuusa
TAMPERE UNIVERSITY OF TECHNOLOGY
Korkeakoulunkatu 3, FI-33101
Tampere, Finland
Tel.: +358 – 401981522
E-Mail: anssi.makinen@tut.fi
URL: www.tut.fi/set

Keywords

«Fault ride through», «Wind energy», «Real time simulation», «Converter control», «Test bench»

Abstract

This paper presents power hardware-in-the-loop (PHIL) laboratory test environment for wind turbine (WT) prototype. The environment utilizes dSPACE and RTDS real time simulators, converter controlled grid emulator (GE) and the prototype. The analysis is carried out using frequency response measurements. The main contribution is the detailed analysis of the grid emulator performance. The main performance limitations are revealed and it is shown that the performance of the GE is dependent on the hardware of the WT prototype in addition to the design of the emulator itself. The comparison of the operation of the GE with open loop and closed loop control modes is carried out. It is shown that the accuracy of the environment is clearly sufficient for symmetrical voltage dips when closed loop control system is used. However, the open loop controlled GE cannot execute correct point of common coupling voltages independent on the operation point of the WT which is relative to the wind conditions. If the GE is controlled at open loop or at closed loop, the network asymmetrical voltage dips are not generated accurately. The reason is that the system bandwidth is not wide enough to execute negative sequence 50Hz component without gain and phase error. However, the accuracy of the PHIL environment is clearly enough for testing the operation of WT control functionalities under asymmetrical network voltages. These functionalities may include PCC voltage balancing or positive sequence reactive power injection.

Introduction

The amount of installed wind turbines (WT) in the electricity network has increased significantly in recent years. In order to ensure the stable operation of power system, the WTs are required to continue their operation during the network abnormalities such as voltage dips, frequency deviations and voltage swells. The control and protection systems of the WT during the abnormalities are designed using offline simulations. However, the practical operation of WT control functions during the abnormalities or faults should be tested in laboratory before installation of the WT [1]. For that purpose, voltage dip generator (VDG) to operate as grid emulator (GE) is needed to generate the faulted voltages to the point of common coupling (PCC) of the WT.

Considering only voltage dips, four different types of VDGs represented in Fig. 1 are used in testing of low voltage ride-through (LVRT) capability of WTs. The dip generators are implemented using generator, shunt impedance, transformer or power electronic converter [2]. The main drawback of the generator-based VDG is the possibility to generate only symmetrical dips. In addition, the realization of the dip takes several grid periods making the operation slow. Shunt impedance based VDG can be effectively used to generate different kinds of voltage dips (1-phase, 2-phase, 3-phase). In [3] and [4], shunt-impedance-based VDG has been used to test 5MW WT and 1.6MW doubly fed induction generator, respectively. However, the drawback of the shunt impedance VDG is the need of adjustable inductors. In addition, controllable generation of harmonics is not possible. In order that the transformer-based VDG operates sufficiently, the same amount of power electronic switches must be used as in the case of converter-based solution. The converter-based solution provides possibility to emulate symmetrical and asymmetrical voltage dips, voltage harmonics as well as voltage swells and flicker. In addition, only converter-based emulator is able to generate frequency deviations. [2] Due to these benefits, the converter-based solution is used in this study to operate as GE.

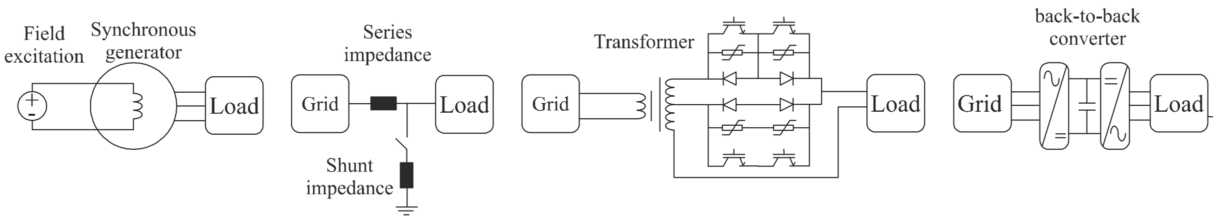

Fig. 1: Four different types of voltage dip generators [1][2]

Although the performance of protection and control systems during the voltage dips can be tested using the aforementioned dip generators, the impacts of the WT operation to power system operation cannot be investigated. However, these impacts can be analyzed using Power hardware-in-the-loop (PHIL) test environment. In PHIL environment, the GE generates voltages to the hardware under test based on the real time simulation of network model. In the model, the measured hardware currents are modelled as current sources. In this study, the hardware under test is WT prototype. In several PHIL applications [5],[6],[7], the simulation of power system is carried out using Real-Time Digital Simulator (RTDS). In [5], the RTDS-simulated PCC voltages are generated using motor-generator combination. However, the response of the voltage generation is slow. In [6], the PHIL system for testing the operation of photovoltaic inverter (PV) is presented. However, the GE was not able to generate unbalanced voltages to the PCC of the PV inverter. In [7], it is shown that PHIL environment can be utilized also at megawatt power level. However, the PCC voltages are not controlled which means that the voltages may not follow the references as the operation point changes.

In this paper, the PHIL environment for WT laboratory prototype is presented. The RTDS simulates network model which is based on real impedances measured from real Finnish network. Inexpensive commercial 10kVA converter with switching frequency of 10 kHz is configured to operate as a GE. The GE and the prototype WT are controlled using two dSPACE real time simulators. The aim of the study is to analyze how well the GE can generate reference voltages determined by the power system model simulated using the RTDS. The performance of the GE operation during the steady state is compared at open and closed loop voltage control modes using frequency response measurements. Time-domain measurements under network symmetrical and asymmetrical voltage dips are also carried out to measure the performance under transients. It is shown that the performance is dependent on the hardware of the tested WT in addition to the design of the emulator itself. This may not be recognized in studies where the GE performance is investigated using only resistive load. [8]

Power hardware-in-the-loop laboratory test environment

The block diagram of the PHIL laboratory test environment for WT prototype is shown in Fig. 2. The DC-motor is used to emulate the operation of WT rotor by producing mechanical torque to the rotor shaft. The operation of the DC-motor is controlled using thyristor rectifier. The rotational frequency of the permanent magnet synchronous WT generator is controlled using self-made three-level three-wire rectifier based on IGBT switches. The WT grid-side converter is self-made three-level four-wire IGBT based converter which controls the DC-link voltage to 750V. The WT generator side converter and the grid side converters are rated at 10 kVA. The current control systems of both WT converters as well as the DC-link voltage control system are implemented using a Freescale MPC563 microcontroller. The aerodynamic model of the WT rotor and the speed control system is simulated using dSPACE. The speed control system aims to optimize the tip speed ratio in order to maximize the power generation under different wind conditions. Based on measured wind speed and rotational frequency of the generator, the aerodynamic model calculates the torque reference for the thyristor rectifier.

The power network, shown in Fig. 3, is modelled in RSCAD software and the RTDS simulates the model in real time. The WT currents are measured and fed to RTDS where the currents are scaled. Thus, the WT is modelled as a current source in the RSCAD model. In this study, the 10kVA WT prototype is scaled to 500kVA in RSCAD model. The PCC voltages from RTDS are scaled from $690V_{l\text{-}l}$ to $329V_{l\text{-}l}$ before transfer to control system of the GE. The outputs of the RTDS are the PCC voltage references ($\underline{u}_{PCC}^{*}$) and the aim of the GE is to generate the reference voltages to the PCC of the WT prototype. The control system of the GE is implemented using second dSPACE whose outputs are the duty cycles for the GE. The hardware of the GE consists of the converter, LC-filter and 400V/400V isolation transformer. The active grid-side converter is needed to allow the power generated by the WT to be transferred into the utility network.

The network model parameters are collected in Table I and wind-turbine-prototype parameters are shown in Table II. The isolation transformer parameters as well as the grid emulator and the grid side converter parameters are depicted in Table III and Table IV, respectively. The hardware arrangement of the PHIL laboratory test setup is depicted in Fig. 4.

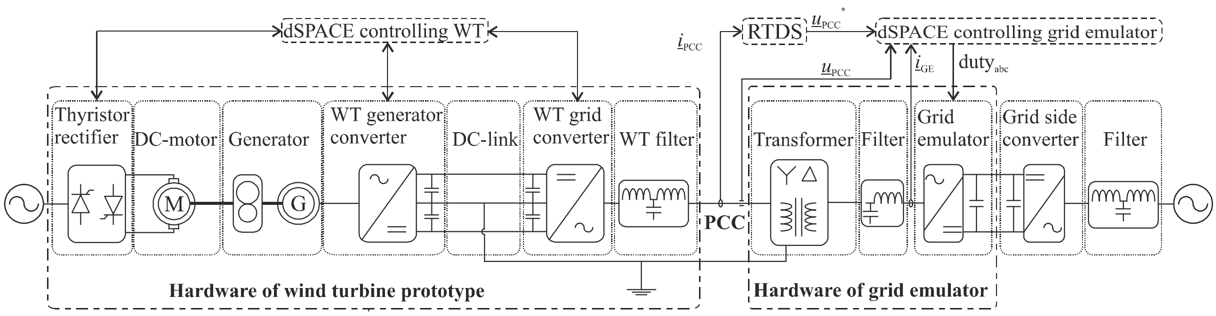

Fig. 2: Block diagram of laboratory test setup

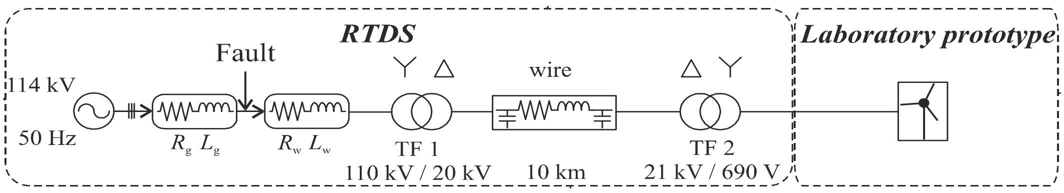

Fig. 3: Network modelled in RSCAD

Table I: Network model parameters

Transformer 1 (TF1)	S_n=16 MVA	U_1/U_2=110/20 kV	L_σ=0.109 pu	no load losses = 0.00336 pu
Transformer 2 (TF2)	S_n=0.6 MVA	U_1/U_2=21/0.69 kV	L_σ=0.03 pu	no load losses = 0.0005 pu
Network impedance	L_g=0.02104 H	R_g=2.513 Ω	L_w=0.041 H	R_w=5.03 Ω

Table II: Wind turbine prototype parameters

Generator						
p = 12	J = 17kgm^2	n_n = 117rpm	T_n = 1800Nm	R_s=0.22Ω	$L_d = L_q$ =9.2mH	ψ = 1.2Wb
Generator side converter 10kVA			Grid side converter 10kVA			
f_{sw}=10kHz	C_{dc}^{+}=1.1mF	C_{dc}^{-}=1.1mF	f_{sw}=10kHz	C_{dc}^{+}=1.1mF	C_{dc}^{-}=1.1mF	U_{dc} = 750V
WT prototype filter						
L_1 = 5mH	L_2 = 0.6mH	C_f=10μF	R_{damp}= 18 Ω (parallel with L_2)			

Table III: Isolation transformer

S_n=50kVA	f_n=50Hz	U_1/U_2=400/400V	L_σ=0.021pu	R=0.043pu	L_m=32.4pu

Table IV: Grid emulator and grid side converter parameters

Grid emulator		Grid side converter		U_{dc} = 650 V
f_{sw} = 10kHz	S_n = 10 kVA	f_{sw} = 3.6 kHz	S_n = 10 kVA	
Grid emulator filter				
L_1 = 2.3mH		C_f = 10 μF		R_{damp} = 2.5Ω (series with capacitor)

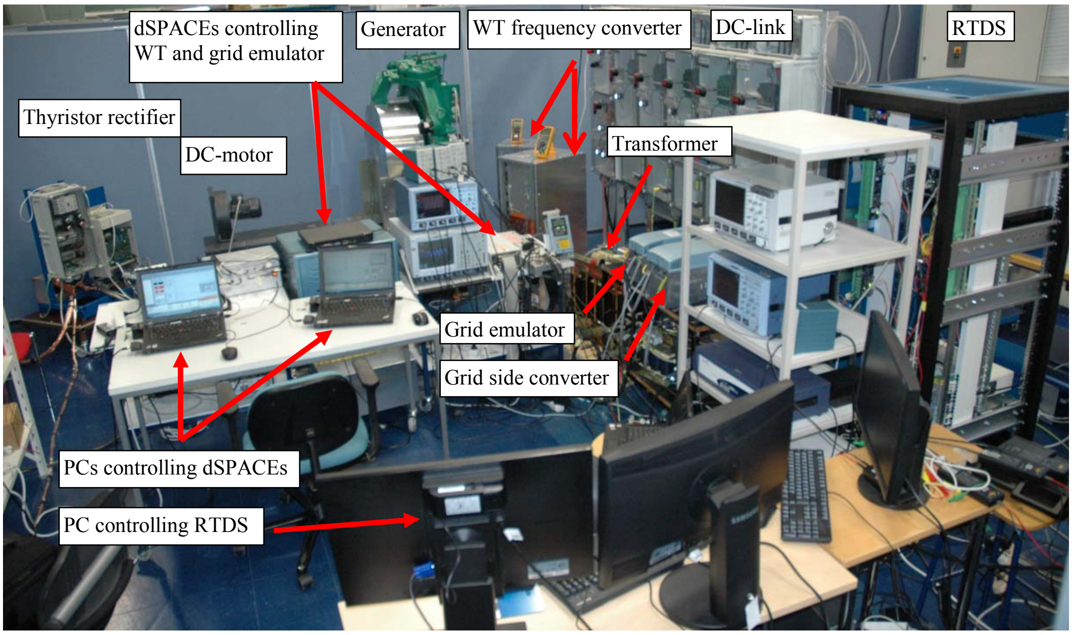

Fig. 4: Hardware arrangement of PHIL laboratory test setup

Control system of grid emulator

The control system block diagram of the GE is shown in Fig. 5. The measured PCC currents are low-pass filtered and fed to RTDS simulation. In this study, two control modes to generate the GE reference voltages $u_{GE,abc}^*$ are compared. In the open loop mode, the $u_{GE,dq}^*$ correspond to RTDS reference voltages $u_{PCC,dq}^*$. The aim of the feedforward term $\Delta\theta$ is to take into account the phase shift caused by the delta/star transformer and the filter impedances. This improves the open loop operation of the GE. In the closed loop control mode, cascaded voltage and current control (VC-control) is used. The outer loop controls the PCC voltages ($\underline{u}_{PCC}$) and the faster inner loop controls the grid emulator currents ($\underline{i}_{GE}$). The measured $u_{PCC,abc}$ and $i_{GE,abc}$ are low-pass filtered before fed to control system. The cut-off frequency of all low-pass filters (LPF) is 700Hz. The control system is implemented in a synchronous reference frame which rotates with the positive sequence component of the PCC reference voltage provided by the RTDS. Dual second order generalized integrator – frequency locked loop (DSOGI-FLL) [9] is used as a synchronizing method. Space vector pulse width modulation (SVPWM) is used to generate duty cycles which are fed from dSPACE to the GE via optical signals.

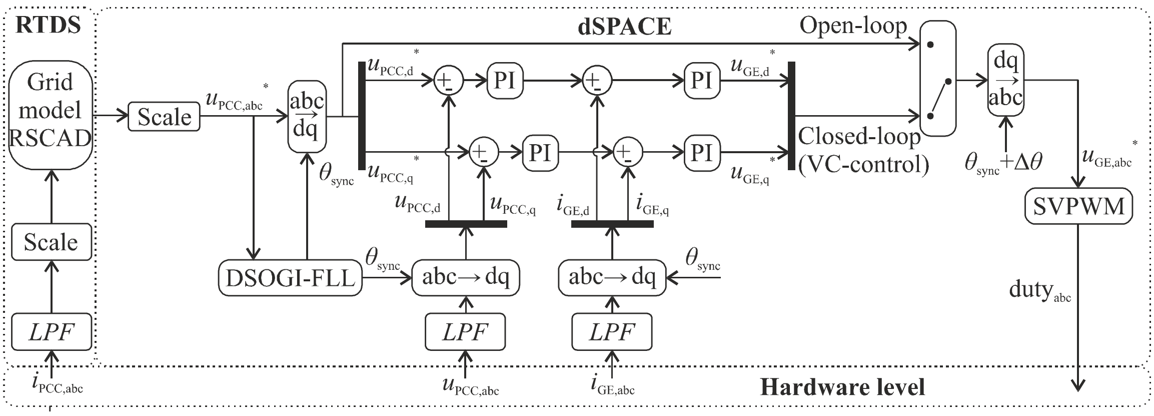

Fig. 5: Control system block diagram of GE

Tuning of controllers

The transfer functions u_d/u_d^* as well as u_q/u_q^* were measured using a frequency response analyzer model 3120 manufactured by Agilent. The wind speed was set to a nominal value of 12m/s during the measurements. The open loop transfer function, i.e. the control loop gain, was calculated from the measured closed loop transfer function in order to measure gain margin GM and phase margin PM. The margins were utilized in the controller tuning process in order to find optimal parameters for PI controllers. With the used PI-controller parameters, the measured open and closed loop transfer functions for d and q-channels are shown in Fig. 6a and Fig. 6b, respectively. The d-channel and the q-channel gain margins are 6,49dB and 7,79dB, respectively. The corresponding phase margins are 82,2 and 82,3 degrees. According to [10], reasonable GM and PM values are GM = 2-5 (2 = 6dB) and PM = 30-60°. Based on the measured GM and PM it can be concluded that the GE performance cannot be improved remarkably by choosing different parameters in PI controllers without compromising the stability of the system. The selected controller parameters are shown in Table V.

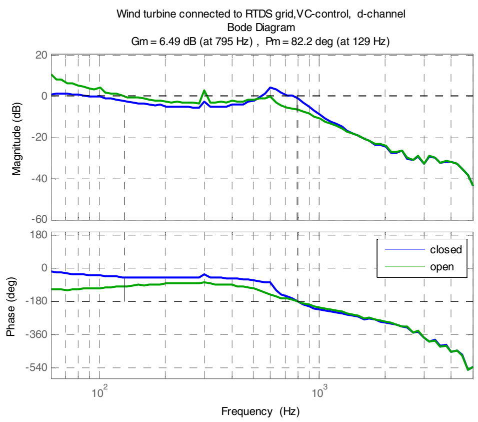

a)

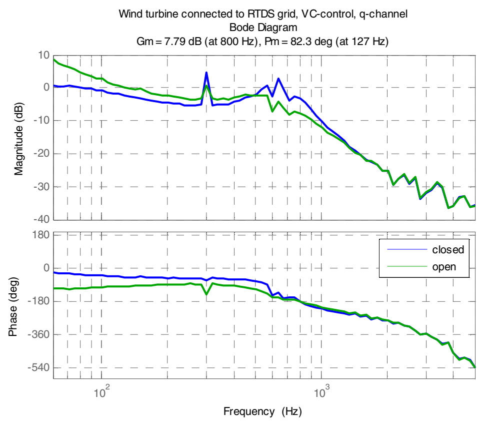

b)

Fig. 6: Measured closed loop transfer functions and control loop gains when wind turbine is connected to grid simulated by RTDS: a) u_d/u_d^*, b) u_q/u_q^*

Table V: Controller parameters

Controller	Voltage		Current	
Parameter	Gain $k = 0.2$	Integrator time $T_i = 3.8$ms	Gain $k = 1.8$	Integrator time $T_i = 0.6$ms

Performance of grid emulator

The system response for positive sequence and negative sequence voltage components is measured in order to assess the performance of the GE. The measurements are realized by adding a small-signal perturbation to the control reference and feeding the reference and the measured PCC voltages to the frequency response analyzer. The frequency analyser then calculates the gain ratio and phase difference between measured and reference component in the injection frequency. In direct current (DC) systems, the injection is added directly to the control reference. However, the measurement of the frequency response of the GE, which is AC system, is not as straightforward as in DC systems. The reason is that the control system is realized in synchronous reference frame oriented to the network voltage vector which rotates typically with the frequency of 50Hz. Thus, injection added to voltage control reference does not generate AC voltage components in the injection frequency. This problem is solved using frequency response arrangement shown in Fig. 7.

The injection is fed to SOGI-FLL [9], [11] which outputs the rotational frequency of the injection signal ω'_{inj}. The angle of the injection θ'_{inj} is obtained after integration. The θ'_{inj} is fed to inverse Park transformation [11] which d-axis input is the peak value of the injection voltage and q-axis input is set to zero. As a result, symmetrical three phase voltages with injection frequency are obtained. Using this arrangement the positive sequence frequency response can be measured. The negative sequence frequency response can be measured if injection voltage $u_{b,inj}$ is added to the $u_{PCC,c}^*$ and $u_{c,inj}$ is added to the $u_{PCC,b}^*$.

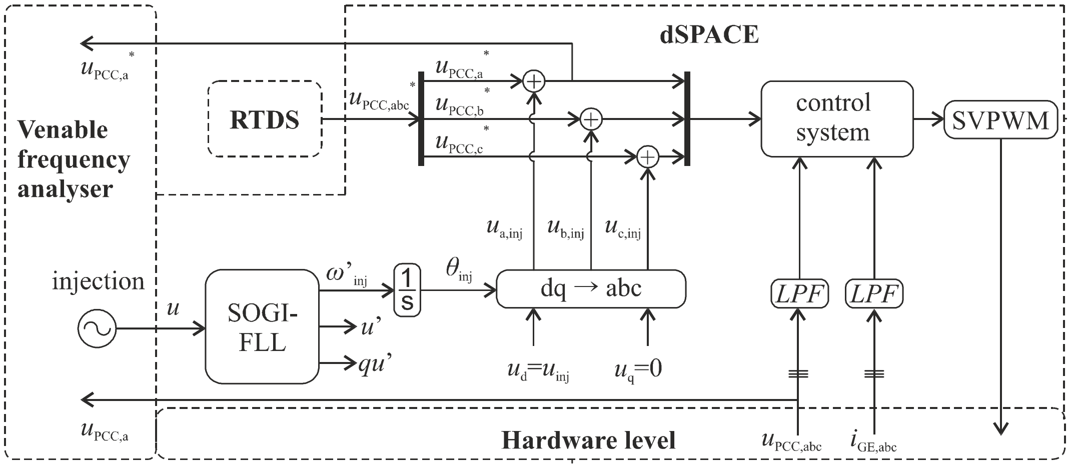

Fig. 7: Positive sequence frequency response measurement arrangement

The measured open loop control mode frequency response of the GE in frequency range of 10Hz – 1300Hz is shown in Fig. 8a and the closed loop frequency response is shown in Fig. 8b. The wind speed was set to 12m/s. The red and blue labels describe the positive and the negative sequence frequency response, respectively. The positive and negative sequence gains and phases are close to unity (0dB) for low frequencies. After 200Hz, the gains start to increase and the phases start to decrease. Critical frequencies from the GE operation performance viewpoint are positive sequence 50Hz and negative sequence 50Hz (-50Hz). If gain and phase are zero at 50 Hz frequency the GE can generate desired reference symmetrical voltages. If the gain and phase are zero also at point -50Hz the unbalanced reference voltages can be executed accurately. The gain and phase values at frequencies 50Hz and -50Hz are 0.6dB, 3°, -0.7dB and -11°, respectively. In practice, the gain 0.6dB means that the peak value of the measured symmetrical phase voltages is around 20V higher than the peak value of the reference voltages. The highest gain in the open loop response is 5dB and it is found approximately at 700Hz which means that the system amplifies mostly voltage components at that frequency. The frequency corresponds to the resonant frequency of the WT filter as shown in Fig. 9a where the bode plot of the WT filter impedance is shown. The bode plot of GE filter impedance including the isolation transformer is shown in Fig. 9b.

When the closed loop control mode is used, the gain and the phase value at positive sequence 50Hz are 0.002dB and 5°. The unity gain value was expected because the main function of the closed loop control system is to eliminate the control error at grid frequency. The phase shift of 5° appears due to the low pass filters of the measurements. The measured gain and phase at -50Hz frequency are incorrect in Fig. 8b. It can be seen that the negative sequence phase jumps to positive sequence value at 50Hz. The incorrect operation appears due to the frequency response measurement arrangement. When the Frequency analyzer is injecting 50Hz component which is transformed to -50Hz component, it calculates the gain and the phase values from the positive sequence 50Hz components. This happens because the positive sequence voltage component at 50Hz is much greater (peak value around 270V) than the negative sequence injection voltages (peak value 6V). However, the correct gain and phase values can be estimated using linear approximation from the values before and after the -50Hz point. The gain and phase values are approximately -0.3dB and -40°.

The bandwidth of the closed loop control mode positive sequence frequency response is approximately 220Hz where the bandwidth is defined as the frequency, at which the frequency response has declined 3dB from 0dB. [12] The bandwidth defined as above is not very useful measure of the accuracy of the GE. More important measure is the frequency range where the control system can generate the reference voltages with gain and phase closely to zero. However, the bandwidth defined as above gives indication on how fast the control system is able to generate the reference values after transient. From the GE operation point of view, the control system is able to generate the reference voltages after symmetrical voltage dip faster as the bandwidth increases.

Again, the peak value of the response appears at around 700Hz. These measurements show that the bandwidth of the closed loop control system is mainly limited by the resonances of the passive reactive components installed in the laboratory setup. In this case, the bandwidth and therefore also the performance of the GE control system is limited by the passive components of the WT prototype. Thus, in general, the performance of GE is dependent on the hardware under test in addition to design of the emulator itself.

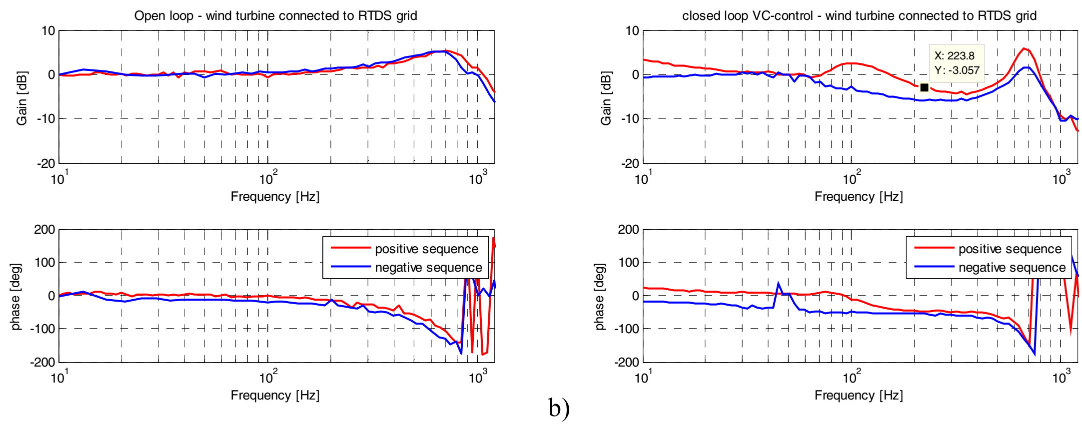

a) b)

Fig. 8: Positive and negative sequence frequency response of the GE: a) open loop mode, b) closed loop mode

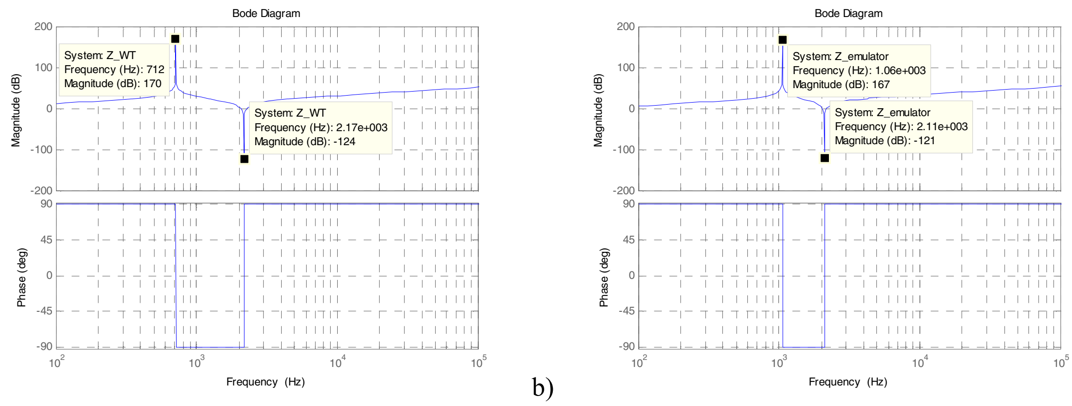

a) b)

Fig. 9: Bode plot: a) Impedance of WT filter, b) impedance of GE including isolation transformer

Laboratory prototype under symmetrical fault

In this section, the operation of the PHIL test setup is studied under symmetrical network fault. The wind speed is 11m/s when three phase fault occurs in network simulated by RTDS, Fig. 3. The reference phase voltages from RTDS and measured voltages from PCC are shown in Fig. 10a when the GE is operating at open loop mode. The fault occurs at 1.51s and endures 100ms. Due to the fact that the PCC voltages are not closed loop controlled, the measured voltages are higher than the reference voltages even during steady state. The reason is the voltage drop over the impedance of the WT filter, the transformer and the GE filter caused by the generated currents by the WT. Thus, it can be concluded that open loop controlled GE cannot execute correct PCC voltages independent on the operation point of the WT which is dependent on wind conditions. The measured WT currents which are transferred to RTDS and scaled are shown in Fig. 10b. The currents increase as a result of the voltage dip due to the operation of the DC-link voltage control of the WT grid side converter.

The reference voltages from RTDS and the measured voltages from PCC are shown in Fig. 11a when the GE is operating at closed loop control mode. The voltage dip occurs at 1.64s. Due to the closed loop control of the PCC voltages the measured voltages correspond to reference values accurately. The high frequency transients in RTDS voltages after the fault cannot be realized by the GE because the control system bandwidth is not infinite. However, it takes approximately 5ms or less from the measured voltages to accurately reach their references. The WT currents after scaling are shown in Fig. 11b. The currents are higher compared to the open loop case. The reason is that the WT prototype is generating same active power with lower PCC voltages. It can be concluded from the results shown in Figs. 11a and 11b that the PHIL environment with closed loop operating GE is clearly accurate enough for the symmetrical low voltage ride through studies and tests.

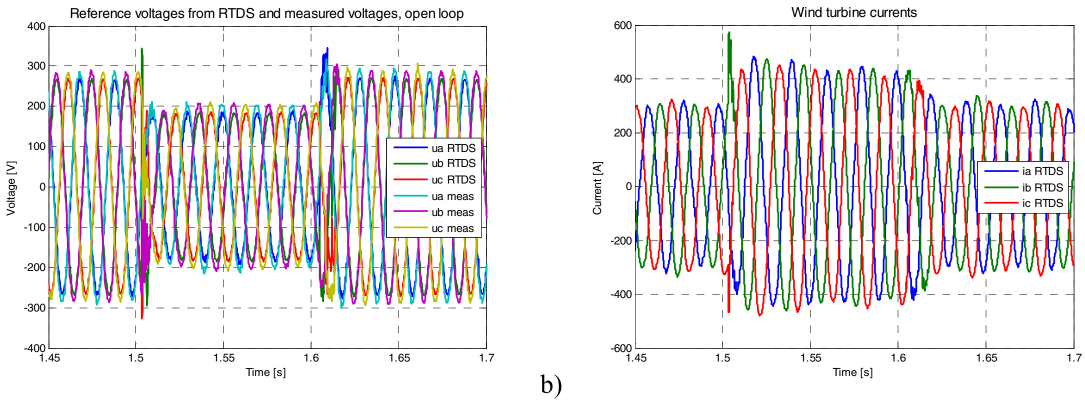

a) b)

Fig. 10: Symmetrical fault in RTDS network during open loop voltage control of the GE: a) reference phase voltages from RTDS and measured phase voltages from PCC, b) measured WT currents after scaling

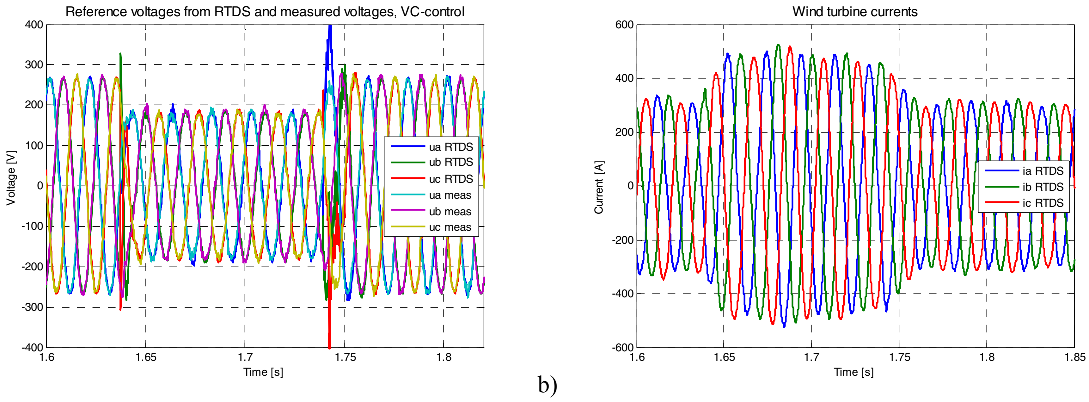

a) b)

Fig. 11: Symmetrical fault in RTDS network during closed loop voltage control of the GE: a) reference phase voltages from RTDS and measured phase voltages from PCC, b) measured WT currents after scaling

Laboratory prototype under asymmetrical fault

In this section, the operation of the PHIL test setup is investigated under asymmetrical network fault. One-phase to earth fault occurs at same network point as in previous case. The RTDS reference voltages and measured voltages are depicted in Fig. 12a when the GE is operating at open loop mode. The wind speed is 11 m/s and the fault occurs at 1.47s. Due to the delta/star transformer in the network model the one phase fault generates two phase voltage dip in the PCC. It can be noticed that all the measured voltages are higher than the references obtained from the RTDS during the fault. The reason is the uncontrolled positive sequence 50Hz voltage component causing the GE to be unable to take into account the operation point of the WT. The wind turbine currents are shown in Fig. 12b. The WT currents increase due to the decrease in positive sequence voltage component in the network voltage due to the fault.

The reference voltages from RTDS and the measured voltages from PCC are shown in Fig. 13a when the GE is operating at closed loop control mode. The fault occurs at 1.595s. The $u_{a,meas}$ correspond to $u_{a,RTDS}$ with decent accuracy during the fault. However, the $u_{b,meas}$ is clearly higher than its reference

$u_{b,RTDS}$ while the $u_{c,meas}$ is lower than $u_{c,RTDS}$. It can be concluded that the GE cannot realize the unbalanced PCC voltages accurately. This is due to the fact that the VC-control system cannot generate perfectly negative sequence 50 Hz voltage component references. This has been illustrated in Fig. 8b. The WT currents are shown in Fig. 13b. Again, the WT currents increase due to the decrease in positive sequence network voltage component. However, the negative sequence network voltage component does not have significant harmonic impact to the currents. The reason is that the DC-link voltage controller and the phase-locked-loop (PLL) controller of the WT prototype are tuned to relatively low bandwidth in order to reject network voltage harmonics.

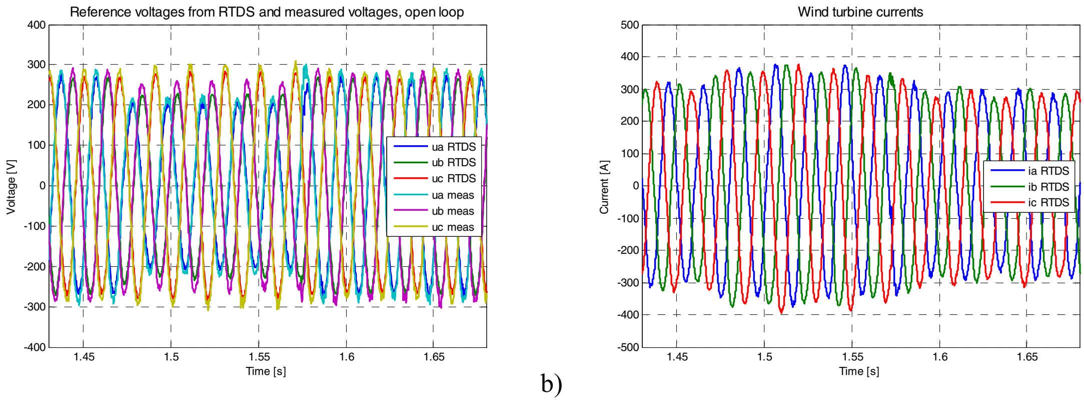

a) b)

Fig. 12: Asymmetrical fault in RTDS network during open loop voltage control of the GE: a) reference phase voltages from RTDS and measured phase voltages from PCC, b) measured WT currents after scaling

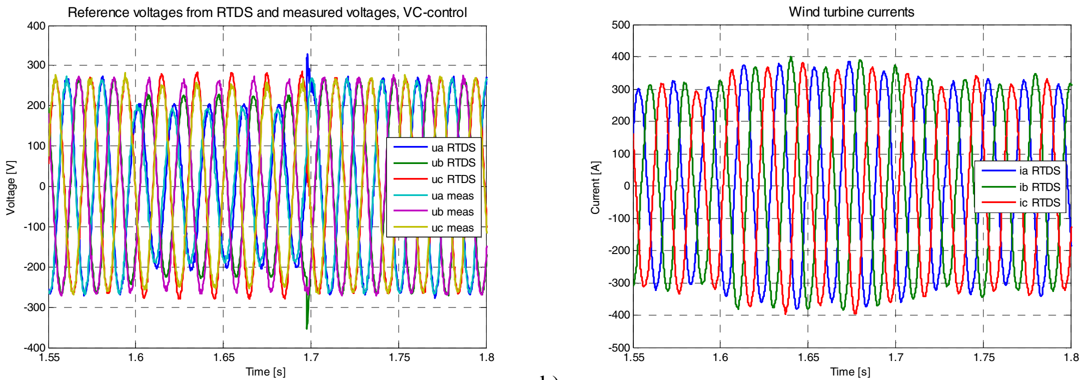

a) b)

Fig. 13: Asymmetrical fault in RTDS network during closed loop voltage control of the GE: a) reference phase voltages from RTDS and measured phase voltages from PCC, b) measured WT currents after scaling

Conclusion

In this paper, PHIL laboratory test environment for WT prototype is presented. The environment can be utilized in WT and grid interaction studies from both the WT and the power system point of views. The environment consists of two dSPACEs, RTDS, converter controlled GE and laboratory prototype of WT. The RTDS simulates the power system network while the dSPACEs are used to control the operation of the GE and the WT prototype. The GE generates voltages to the PCC of the laboratory prototype WT based on the network model simulated by the RTDS. The WT prototype currents are measured and fed back to the RTDS model.

The main contribution of the paper is the detailed analysis of the performance of the GE. The analysis is carried out using frequency response measurements. The main performance limitations are revealed and it is shown that the performance of the GE is dependent on the hardware of the WT prototype in addition to the design of the emulator itself. The comparison of the operation of the GE with open loop and closed loop control modes is carried out. The closed loop control parameters are selected based on the measured gain and the phase margins. The operation of the PHIL environment under symmetrical and asymmetrical network voltage dips is tested. It is shown that the accuracy of the environment is clearly sufficient for symmetrical LVRT tests when closed loop control system is used. However, the open loop controlled GE cannot execute correct PCC voltages independent on the operation point of the WT which is dependent on the wind conditions. If the GE is controlled at open loop or closed loop the network asymmetrical voltage dips are not generated accurately. The reason is that the control system bandwidth is not wide enough to execute negative sequence 50Hz component without gain and phase error. However, the accuracy of the PHIL environment is clearly enough for testing the operation of WT control functionalities under asymmetrical network voltages. These functionalities may include PCC voltage balancing or positive sequence reactive power injection.

References

[1] R. Pöllänen, L. Kankainen, M. Pääkkönen, J. Ollila, S. Strandberg, ”Full-power converter based test bench for low voltage ride-through testing of wind turbine converters”, 14th European Conference on Power Electronics and Applications, EPE 2011, Birmingham, Great Britain, 10p.

[2] C. Wessels, T. Wehrend, F.W. Fuchs, “Transformer based voltage sag generator to test renewable energy systems during grid faults in the laboratory”, EPE Wind Energy Chapter Symposium, April 2010, 8p.

[3] M. Garcia-Gracia, M. P. Comech, J. Sallan, D. Lopez-Andia, O. Alonso, “Voltage dip generator for wind energy systems up to 5MW”, Applied Energy, vol. 86, no. 4, 2009, pp. 565 – 574.

[4] J. Niiranen, “Experiences on voltage dip ride through factory testing of synchronous and doubly fed generator drives”, European Conference on Power Electronics and Applications, EPE 2005, Dresden, Germany, 11 p.

[5] A.J. Roscoe, A. Mackay, G.M. Burt, J.R. McDonald, “Architecture of a network-in-the-loop environment for AC power-system behaviour”, IEEE Transactions on Industrial Electronics , Vol. 57, No. 4, April 2010, pp. 1245-1253.

[6] P. Kotsampopoulos, V. Kleftakis, G. Messinis, N. Hatziargyriou, ”Design, development and operation of a PHIL environment for distributed energy resources”, 38th Annual Conference on IEEE Industrial Electronics Society, IECON 2012, Montreal, Canada, pp. 4765-4770.

[7] M. Steurer, C. S. Edrinton, M. Sloderbeck, W. Ren, J. Langston, “A megawatt-scale power hardware-in-the-loop setup for motor drives”, IEEE Transactions on Industial Electronics, Vol. 57, No. 4, April 2010, pp. 1254-1260.

[8] R. Lohde, F.W Fuchs, ”Laboratory type PWM grid emulator for generating disturbed voltages for testing grid connected devices”, 13th European Conference on Power Electronics and Applications, 2009, EPE 2009, Barcelona, Spain, 9p.

[9] A.S. Mäkinen, H. Tuusa, “Analysis, comparison and performance evaluation of wind turbine grid synchronizing methods”, IEEE International Conference on Computer as a Tool (EUROCON’13), Zagreb, Croatia, July 1-4, 2013, 8p.

[10] K.J. Åström and T. Hägglund, “Advanced PID control”, ISA- Instrumentation, Systems and Automation Society, United States, 2006, 460p.

[11] R. Teodorescu, M. Liserre, P. Rodriquez, “Grid converters for photovoltaic and wind power systems”, John Wiley & Sons, Ltd., 2011, 398p.

[12] R.C Dorf and R.H. Bishop, “Modern control systems – ninth edition”, Prentice –Hall, Inc, Upper Saddle River, New Jersey, United States, 2001, 831p.